Available online at www.eccomasproceedia.org
Eccomas Proceedia COMPDYN (2025) 2984-2995

ECCOMAS
Proceedia

COMPDYN 2025
10th ECCOMAS Thematic Conference on
Computational Methods in Structural Dynamics and Earthquake Engineering
M. Papadrakakis, M. Fragiadakis (eds.)
Rhodes Island, Greece, 15-18 June 2025

SEISMIC FRAGILITY OF A STOCK OF UNBRACED PALLET RACKS CONSIDERING EVENTS ON AMPLIFYING SOILS

Marco Donà[1,2,3], Alberto Zonta[1], Enrico Bernardi[4], Giacomo Piredda[1], Francesca da Porto[1]

[1] Department of Geosciences, University of Padova, Via Gradenigo 6, 35131, Padova, Italy
e-mail: marco.dona.1@unipd.it
alberto.zonta@dicea.unipd.it
giacomo.piredda@iusspavia.it
francesca.daporto@unipd.it

[2] Department of Cultural Heritage, University of Padova, Piazza Capitaniato 7, 35131 Padova, Italy

[3] Department of Information Engineering, University of Padova, Via Gradenigo 6/b, 35131 Padova, Italy

[4] National Research Council, Construction Technologies Institute (CNR-ITC), Via Lombardia 49, 20098 San Giuliano Milanese, Italy
e-mail: {bernardi}@itc.cnr.it

Abstract

Recent seismic events in Italy highlighted the considerable vulnerability of industrial pallet racks that were originally designed solely for gravity loads. Despite this, such racks continue to be the predominant storage solution in industrial settings. This research focuses on assessing the seismic fragility of these systems to support more precise risk evaluations for enterprises and inform the design of effective retrofit strategies. For this purpose, three-dimensional non-linear finite-element models of various unbraced pallet rack configurations—typical of those found in Italy—were analysed through Time-History simulations using many bidirectional ground motion records representative of the Italian seismicity on amplifying soils. Fragility curves were then derived employing various engineering demand parameters and seismic intensity measures within a cloud-based analysis framework.

Keywords: industrial pallet racks; non-linear finite element rack models; time-history analysis; cloud analysis; seismic fragility models

Peer-review under responsibility of the organizing committee of COMPDYN 2025.
doi: 10.7712/120125.12627.25251

1 INTRODUCTION

In recent years, the increasing growth of globalization and e-commerce has significantly driven the demand for goods storage systems. Among these, standard adjustable steel pallet racks are the most commonly used in commercial and logistics facilities. These racks are typically made by assembling cold-formed steel profiles with thin-walled sections, which helps minimise both production costs and time.

Pallet racks are particularly vulnerable to seismic actions due to the combined effects of substantial service live loads, the presence of semi-rigid beam-to-column (*btc*) connections, the limited or absent ductility of their open-section profiles, and the pronounced slenderness of their steel members. In Italy, the seismic weakness of these storage systems became evident during the 2012 Emilia-Romagna and 2016 Central Italy earthquakes [1]. These events also underscored the significant impact of pallet racks on companies' economic losses, primarily driven by business interruptions [2].

Research in this field covered multiple levels of investigation, ranging from the in-depth analysis of the mechanical behaviour of individual rack components and their connections to the assessment of the global seismic response of entire rack systems, using both experimental and numerical approaches. Experimental studies by Padilla-Llano et al. [3 ,4] investigated buckling mechanisms in cold-formed steel members under cyclic axial and flexural loading. The cyclic behaviour of *btc* connections—critical to understanding the lateral response of pallet rack systems—were also examined by various researchers (e.g., [5, 6]). Comprehensive investigations into the seismic performance of storage racks were carried out in the SEISRACKS [7] and SEISRACKS2 [8] experimental campaigns, which combined component-level and full-rack testing with numerical simulations. The SEISRACKS project was developed following the guidelines of FEM Document 10.2.08 [9], while SEISRACKS2—which included a broader range of component and system tests—played a pivotal role in shaping the EN 16681 standard [10].

Collectively, previous studies underscored the significant seismic vulnerability of pallet rack storage systems. In response, several technological solutions were proposed in recent years to enhance their seismic performance. These include the implementation of base isolation systems (e.g., [11]), the integration of specialised energy-dissipating devices (e.g., [12]), and the adoption of load-level isolation strategies (e.g., [13, 14]).

However, only a limited number of studies specifically addressed the seismic fragility of steel pallet racks. Notably, Gabbianelli et al. [15] evaluated conditional fragility curves based on spectral acceleration (S_a) for two common Italian rack typologies—unbraced and braced—using two-dimensional finite element (FE) models in the down-aisle direction and a multiple-stripe analysis method. More recently, Nuñez et al. [16] developed fragility functions for four Chilean archetypes, including squat-unbraced and slender-braced configurations with varying span lengths, employing three-dimensional FE rack models and an incremental dynamic analysis approach. These studies highlight the existing gap in seismic fragility assessments for pallet racks and emphasise the need for further research in this area.

Building upon the methodology proposed by Donà et al. [17], this study extends the seismic fragility assessment of a stock of 27 unbraced pallet racks—characterised by variations in upright sections (U), load level heights (h), and total heights (H), and representative of typical Italian configurations—by considering ground motions on amplifying soil conditions rather than rigid soil (as in the previous study). A cloud-based analysis approach, coupled with refined non-linear 3D FE modelling, was adopted to simulate the rack seismic response. Each rack model was subjected to time-history analyses using 268 bidirectional ground motion records on amplifying soils representative of Italian seismicity. To support the large-scale parametric investigation, a dedicated routine was developed within the OpenSees environment. Fragility curves were derived for multiple engineering demand parameters (EDPs)—namely, total upright strain, inter-level drift, and rotations at beam-to-column and base connections—conditioned on two intensity measures (IMs): spectral acceleration (S_a) and peak ground acceleration (PGA).

2 PARAMETRIC ANALYSIS FRAMEWORK

2.1 Stock of analysed racks

The structural stock examined in this study comprises 27 unbraced, standard adjustable steel pallet racks, designed solely for gravity loads and representative of commonly adopted storage systems in Italy. Specifically, nine geometric configurations (Figure 1) combined with three upright types (U_1, U_2, U_3) were analysed.

All racks share the plan configuration shown in Figure 2a, consisting of seven longitudinal spans of 2700 mm and two transverse frames, each 1000 mm wide and spaced 300 mm apart. The rack variants differ in terms of upright cross-section type (U_1, U_2, U_3), load-level height (h_1 = 1.0 m, h_2 = 1.5 m, h_3 = 2.0 m), and total height (H_1 = 6 m, H_2 = 9 m, H_3 = 12 m), with each configuration defined by a unique combination of these parameters. Each of the three total heights is associated with a distinct transverse frame type, as shown in Figure 2b.

The pallet load was defined according to the load-bearing capacity of the transverse frame, which depends on the upright type, load-level height, and frame width. As a result, for each upright profile, the applied load is governed solely by the values of h and the number of load levels. This approach ensures that all rack configurations develop comparable compressive stresses at the base of the uprights, allowing for a consistent assessment of seismic fragility across a uniform set of structures. Among the three load configurations recommended by EN 16681 [10] for seismic verification, the full-load condition was adopted in this study, as it represents the most demanding scenario for a comprehensive fragility evaluation.

The rack profiles feature open and thin cross-sections, which typically fall into Class 3 or 4 according to EN 1993 [18]. For Class 3 sections, the full material strength can still be used; whereas, Class 4 sections require the use of effective properties due to their susceptibility to buckling phenomena. As illustrated in Figure 2c, the cross-sections considered in this study include Class 3 profiles for the pallet beams, while uprights and bracing members belong to Class 4. Therefore, the stiffness-related properties of the latter were reduced in accordance with EN 15512 [19] to account for local and distortional buckling effects, which were not explicitly simulated. Conversely, global buckling of the uprights was directly evaluated into the numerical modelling approach (see Section 2.2).

In order to accurately simulate the structural behaviour of the racks, the cross-sectional properties of the diagonal elements were reduced, in accordance with the recommendations of EN 15512 [19]. This adjustment reflects the effective stiffness of the frame, which is diminished due to the inherent clearances in the connections of bracing elements. Furthermore, to incorporate the interaction between axial and bending stresses in a model that treats the various section responses independently (see Section 2.2), a reduction in the flexural capacity of the uprights was implemented. This reduction, which is related to the axial compression ratio (i.e., the vertical load relative to the axial capacity of the cross-section), and thus varies with h, was set at 40%, 35%, and 30% for h values of 1.0 m, 1.5 m, and 2.0 m, respectively. As an example, Figure 3 shows a view of the 3D FE model for three case study racks.

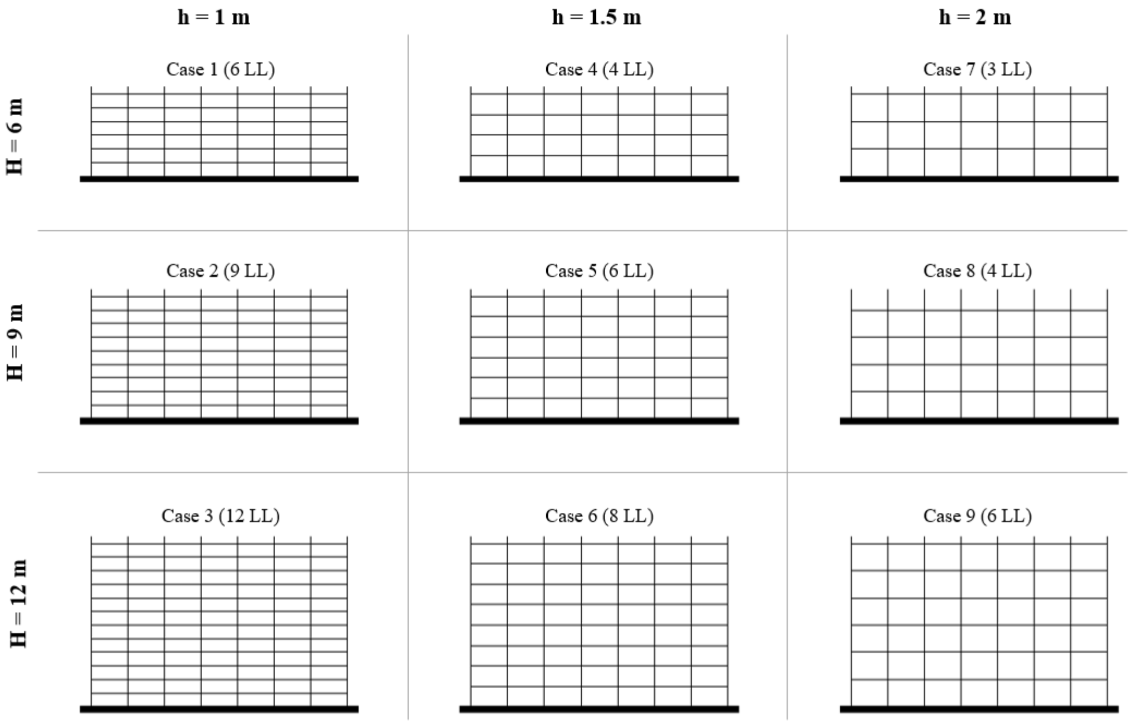

Figure 1: Geometric configurations of case study racks analysed for each upright type (U_1, U_2, U_3).

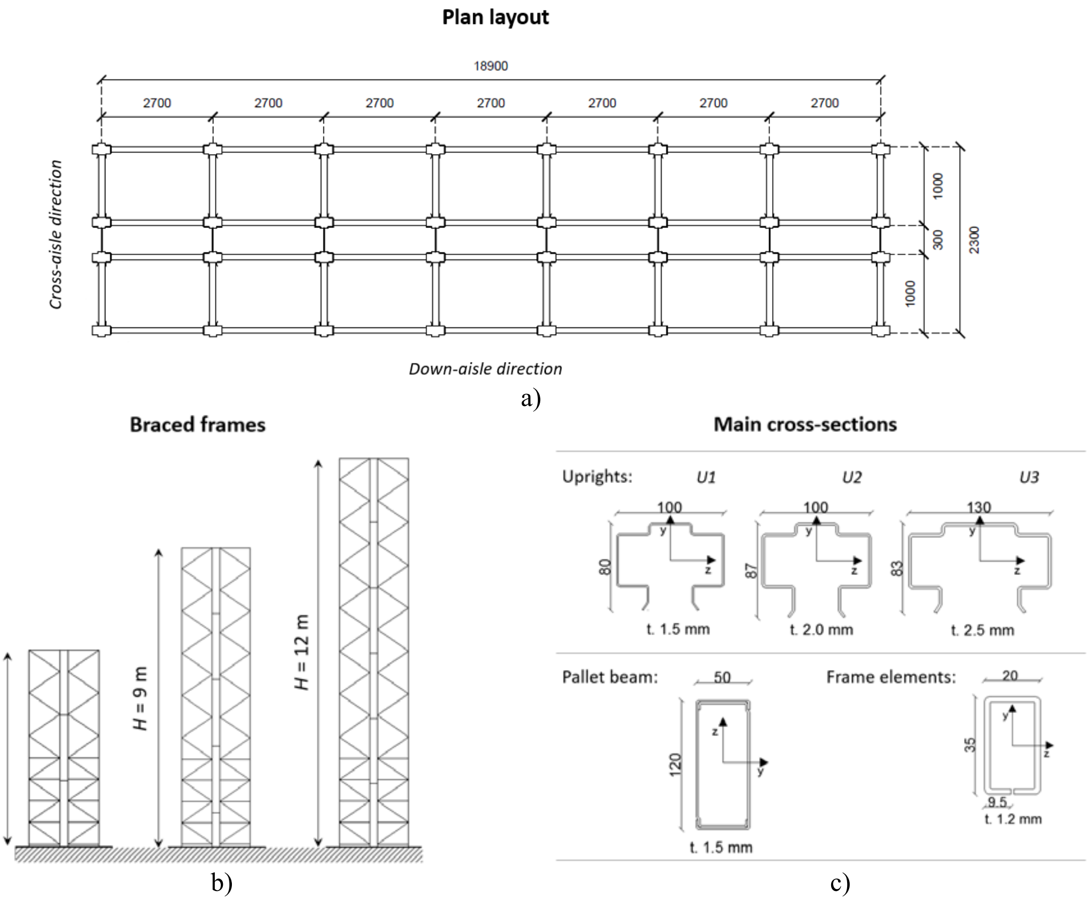

Figure 2: a) plan layout of all racks; b) three frame types (*H_1*, *H_2*, *H_3*); cross-sections analysed.

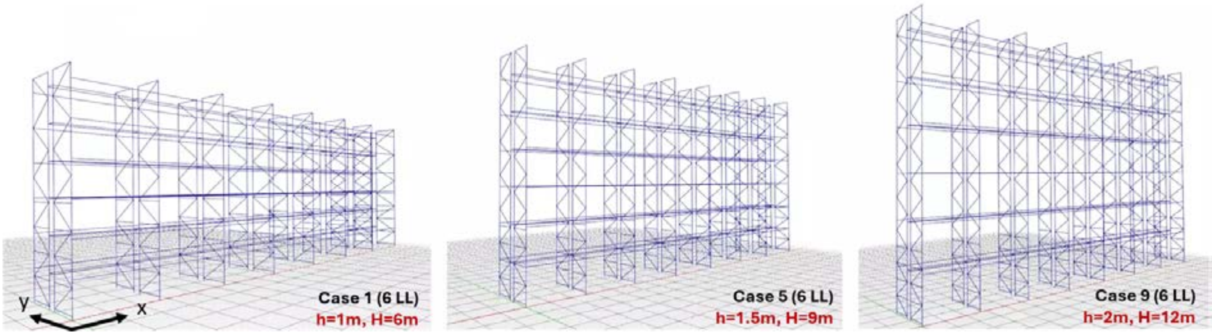

Figure 3: View of the 3D FE model for three case study racks.

2.2 Non-linear rack modelling approach

A customised procedure was developed within the OpenSees framework [20] to effectively assess the fragility of these structures. This procedure automates the generation of 3D non-linear FE rack models, which are then subjected to TH analysis.

The material non-linearities are modelled in distinct ways for each element of the rack system. For the uprights, axial and flexural responses are represented using spread plasticity, whereas for the base and *btc* connections, concentrated plasticity is adopted. In contrast, pallet beams and spacers are modelled as linear elastic components. The pallet loads are placed atop a dummy pyramidal substructure, which allows the correct positioning of the centre of gravity of the pallets in the analysis. Moreover, a friction contact element is employed beneath the pallets to simulate potential sliding along the cross-aisle direction once the friction force ($F_{friction}$) is surpassed. This friction force is calculated as the product of the pallet weight and the friction coefficient μ_s (0.37 for wood-to-steel contact, as specified in EN 16681 [10]).

Table 1 provides a summary of the OpenSees objects used in the modelling of the racks, along with brief descriptions of the section behaviours and material laws applied. The main material laws are then shown in Figure 2. Further details on the structural models of the pallet racks can be found in Donà et al. [17].

Rack elements	OpenSees objects and material laws
Uprights	*Force-Based Beam-Column Elements* Hysteretic asymmetrical axial behaviour via "*uniaxialMaterial Pinching4*" (Figure 4a), accounting for buckling. Elasto-plastic flexural behaviour. Five integration points per element.
Frame bracing elements	*Beam With Hinges Elements* Linear elastic beams with equivalent stiffnesses and end hinges to simulate truss-like behaviour.
Pallet beams/ Spacers	*Elastic Beam Column Elements* Linear elastic beams with equivalent stiffnesses.
Btc and base connections	*Zero-Length Elements* -*Btc*: hysteretic rotational behaviour around Y via "*uniaxialMaterial Hysteretic*" (Figure 4b); linear elastic rotational behaviour around Z; rotation around X equal to that of the beam. -Base: hysteretic rotational behaviour around Y via "*uniaxialMaterial Hysteretic*" (Figure 4c); released rotational stiffness around X; rotation around Z equal to that of the upright.
Mass substructures	*Elastic Beam Column Elements* Linear elastic beams simulating truss behaviour, without affecting modal results.
Pallet-beam contact	*Zero-Length Element* Equivalent friction model (Figure 4d) with penalty stiffness and perfectly plastic behaviour.

Table 1: OpenSees objects employed in pallet rack modelling

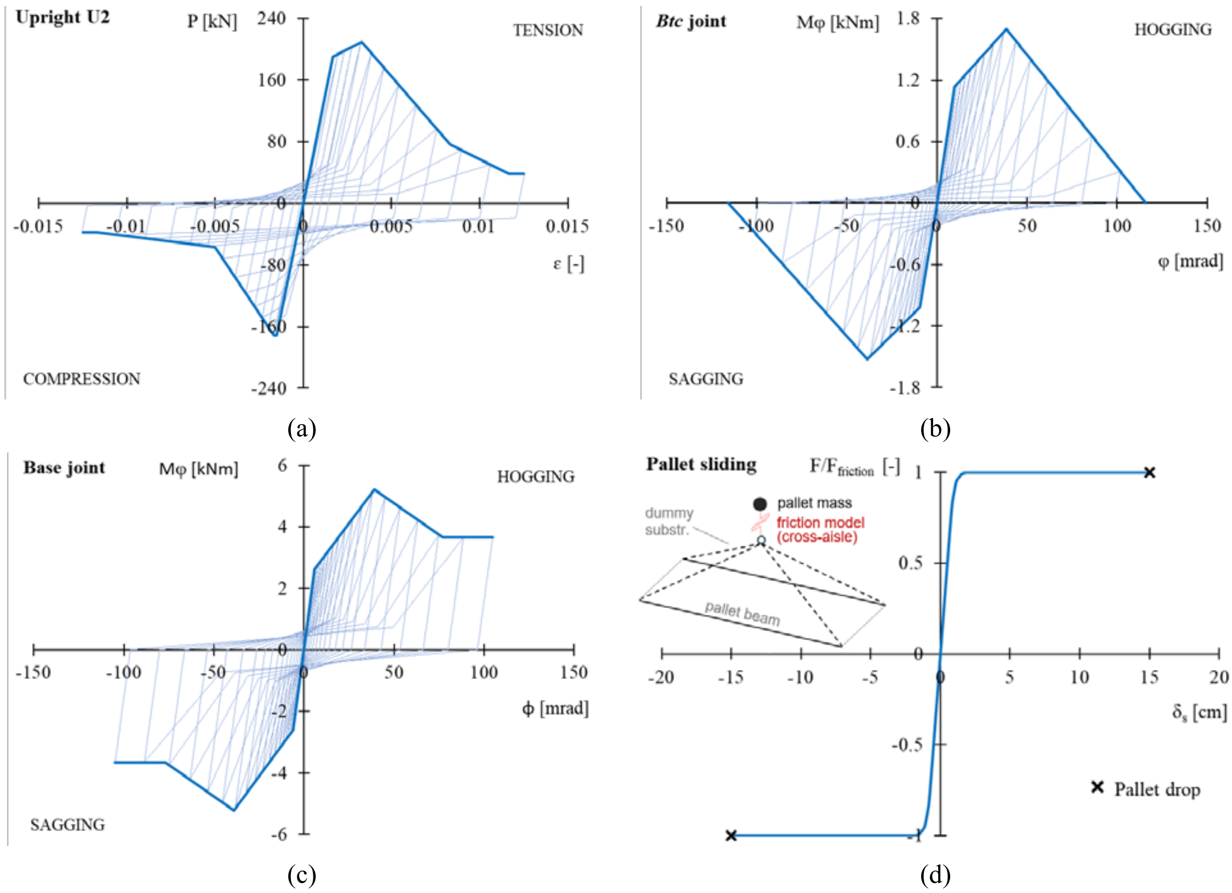

Figure 4: Main constitutive laws for (a) uprights, (b) *btc* joints, (c) base joints, and (d) pallet-beam contact.

3 SEISMIC FRAGILITY APPROACH

To derive the seismic fragility functions from the TH results, a cloud analysis approach was adopted. A dataset of 134 unscaled bidirectional ground motion records, representative of Italian seismicity with amplifying soils, was used ([21, 22]). The peak ground acceleration (PGA) values for the two horizontal components (H_{c1} and H_{c2}) of each ground motion are illustrated in Figure 5a. For each seismic event, two analyses were conducted—first applying the H_{c1} component in the down-aisle (*X*) direction and then in the cross-aisle (*Y*) direction—resulting in a total of 268 simulations per rack configuration, amounting to 7,236 analyses overall. Figure 5b presents the spectral acceleration (S_a) values corresponding to the fundamental periods of the racks in both main directions ($T_{1,X}$, $T_{2,Y}$).

To evaluate the damage level in a structural system, it is essential to establish appropriate damage or performance indicators—commonly referred to as Engineering Demand Parameters (EDPs)—along with their corresponding threshold values that delineate various damage states (DSs) of increasing severity. In this study, four EDPs were adopted: a global strain parameter for the uprights (ε^*), the peak load-level drift in the down-aisle direction (θ_X), and the maximum rotation experienced by the beam-to-column (φ_{btc}) and base (φ_{base}) connections about the *Y*-axis. As defined in Equation (1), ε^* is computed as the sum of three ratios: the actual axial strain (ε_p) over the reduced yield axial strain ($\varepsilon_{p,y} \cdot \chi_P$)—where χ_P is the buckling factor—and the actual curvatures around the local *Y* and *Z* axes (χ_Y, χ_Z) over their respective yield curvatures ($\chi_{Y,y}$, $\chi_{Z,y}$).

Each EDP was associated with three distinct damage states, labelled DS1, DS2, and DS3. DS1 corresponds to the initiation of damage, where the rack system maintains an overall elastic behaviour. DS2 reflects the onset of yielding, a condition in which user safety is still ensured—comparable to the Life Safety limit state. DS3 indicates a critical damage condition where user safety can no longer be guaranteed, and there is a significant risk of progressive failure leading to partial or complete collapse of the rack. The threshold values defining these damage states for each EDP are provided in Table 2

The median ($\mu_{DS,i}$) and logarithmic standard deviation ($\beta_{DS,i}$) of the assumed lognormal cumulative density function were derived using the method of moments, following the approach described by Saler et al. [23]. To ensure an accurate estimation of rack failure probability, analyses that did not converge were also taken into account, as recommended by Jalayer et al. [24]. In this context, structural collapse was considered to occur under two independent scenarios: (*i*) numerical convergence (*Conv*) is achieved, and ε^* reaches or exceeds its DS3 threshold; or (*ii*) the analysis fails to converge (*NoC*), suggesting potential collapse. Accordingly, the collapse probability was computed using the total probability theorem, as shown in Equation (2). It was conservatively assumed that the probability of reaching DS3 given a non-convergent analysis (P($D \geq DS3$ | *IM*, *NoC*)) equals 1, while the likelihood of non-convergence given an intensity measure (P(*NoC* | *IM*)) was estimated through a logistic regression model, described in Equation (3).

$$\varepsilon^* = \frac{\varepsilon_P}{\left(\varepsilon_{P,y} \cdot \chi_P\right)} + \frac{\chi_Y}{\chi_{Y,y}} + \frac{\chi_Z}{\chi_{Z,y}} \tag{1}$$

$$\begin{aligned} P\left(D \geq DS_3 \mid IM\right) = P\left(D \geq DS_3 \mid IM,\ Conv\right) \cdot \left(1 - P\left(NoC \mid IM\right)\right) + \\ + P\left(D \geq DS_3 \mid IM,\ NoC\right) \cdot P\left(NoC \mid IM\right) \end{aligned} \tag{2}$$

$$P\left(NoC \mid IM\right) = \frac{1}{1 + e^{-\left(\alpha_0 + \alpha_1 \cdot \ln\left(IM\right)\right)}} \tag{3}$$

EDP	DS1	DS2	DS3
ε^*	[0.8, 1.0 [	[1.0, 1.5 [	[1.5, +∞ [
$\theta_X / \theta_{X,y}$	[0.8, 1.0 [	[1.0, 1.5 [	[1.5, +∞ [
$\varphi_{btc} / \varphi_{btc,y}$	[0.8, 1.0 [	[1.0, 4.0 [	[4.0*, +∞ [
$\varphi_{base} / \varphi_{base,y}$	[0.8, 1.0 [	[1.0, 6.5 [	[6.5*, +∞ [

"parameter,y" = yield value of specific parameter; "" = peak value of specific EDP*

Table 2. Definition of DSs for the selected EDPs.

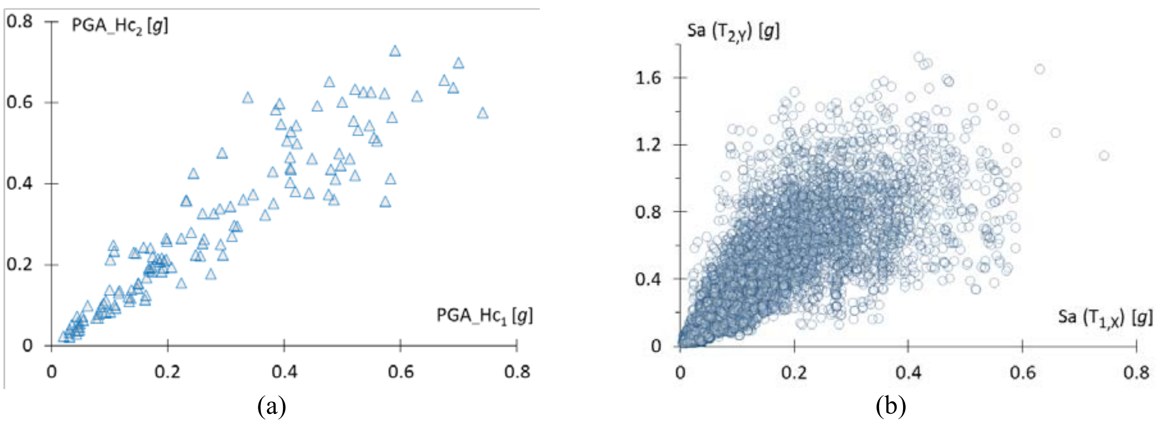

Figure 3: Information on selected bidirectional records: (a) PGA values; (b) Sa values.

4 SEISMIC FRAGILITY MODELS

Given the use of bidirectional ground motion records, careful consideration was required when evaluating the correlation between EDPs and IMs. The parameters θ_X, φ_{btc}, and φ_{base} represent deformations occurring along the down-aisle (*X*) direction and were therefore correlated with IM values in that same direction. On the other hand, ε^*, being a strain parameter influenced by axial force and biaxial bending, does not have an obvious directional association with a specific IM. However, due to the significantly greater stiffness of the analysed unbraced racks in the cross-aisle direction compared to the down-aisle direction—resulting in higher seismic accelerations and inertial forces along the *Y* axis—ε^* was associated with IM values in the *Y* direction.

Figures 4 and 5 present the developed fragility models for the entire rack stock with respect to the selected EDPs, using PGA and S_a as conditioning IMs, respectively. In addition to DS1, DS2, and DS3, the fragility curves representing the probabilities of non-convergence (*NoC*) and actual collapse (*Collapse*) are also displayed in the fragility model based on ε^*. For comparison, the *Collapse* curve—obtained by analysing ε^*—is also included in the fragility plots of the other EDPs.

The key insights from Figure 4 are summarised below.

- The fragility expressed in terms of ε^* exhibits relatively low median PGA values (μ_{PGA}), highlighting the significant seismic vulnerability of these rack systems. The small difference in μ_{PGA} between DS2 (0.088g) and *Collapse* (0.097g) indicates limited structural redundancy and ductility. Furthermore, the proximity of the fragility curves for DS3 (collapse with convergence) and *NoC* (non-convergence) suggests that non-convergence is likely triggered by excessive deformation in the uprights.
- The *Collapse* curve associated with ε^* consistently precedes the DS3 curves of the other EDPs (θ_X, φ_{btc}, and φ_{base}), suggesting that ε^* is the primary performance parameter driving rack failure. Among the remaining EDPs, θ_X is the first to reach the DS3 threshold, making it the most representative indicator of global rack deformation along the down-aisle direction.
- The median PGA values of the *Collapse* curve for ε^* and the DS2 curve for θ_X are very similar, indicating comparable probabilities of upright failure and yielding in the down-aisle direction. When comparing φ_{btc} and θ_X, φ_{btc} exhibits lower median PGA values for DS1 and DS2, but higher values at DS3. This behaviour highlights a rapid reduction in inter-storey stiffness in the X direction following the yielding of the *btc* connections. The base joints (φ_{base}) display the lowest fragility: DS1 is reached only after DS2 has been reached for both θ_X and φ_{btc}, and DS3 is never attained. This suggests a hierarchy in the resistance capacities of the various structural components of these racking systems.

As shown in Figure 5, while the significant acceleration ranges for fragility in terms of PGA and S_a remain comparable for ε^*, these ranges are significantly reduced for the other EDPs when transitioning from PGA to S_a. For example, for the *Collapse* curve, μ_{Sa} is 0.111g, which is comparable with the relevant μ_{PGA} value (0.097g). Instead, for the DS2 curves of φ_{btc}, θ_X, and φ_{base}, the values of μ_{PGA} vs. μ_{Sa} are respectively 0.083g vs. 0.035g, 0.104g vs. 0.043g, and 0.143g vs. 0.060g. This reduction is attributed to the long vibration periods characterising these racks in the down-aisle direction. In this context, since the *Collapse* curve is defined using S_a values in the *Y* direction—i.e., derived from the main vibration period of racks in the cross-aisle direction—it is no longer directly comparable to the fragility curves of θ_X, φ_{btc}, and φ_{base}, although it can still serve as a useful reference.

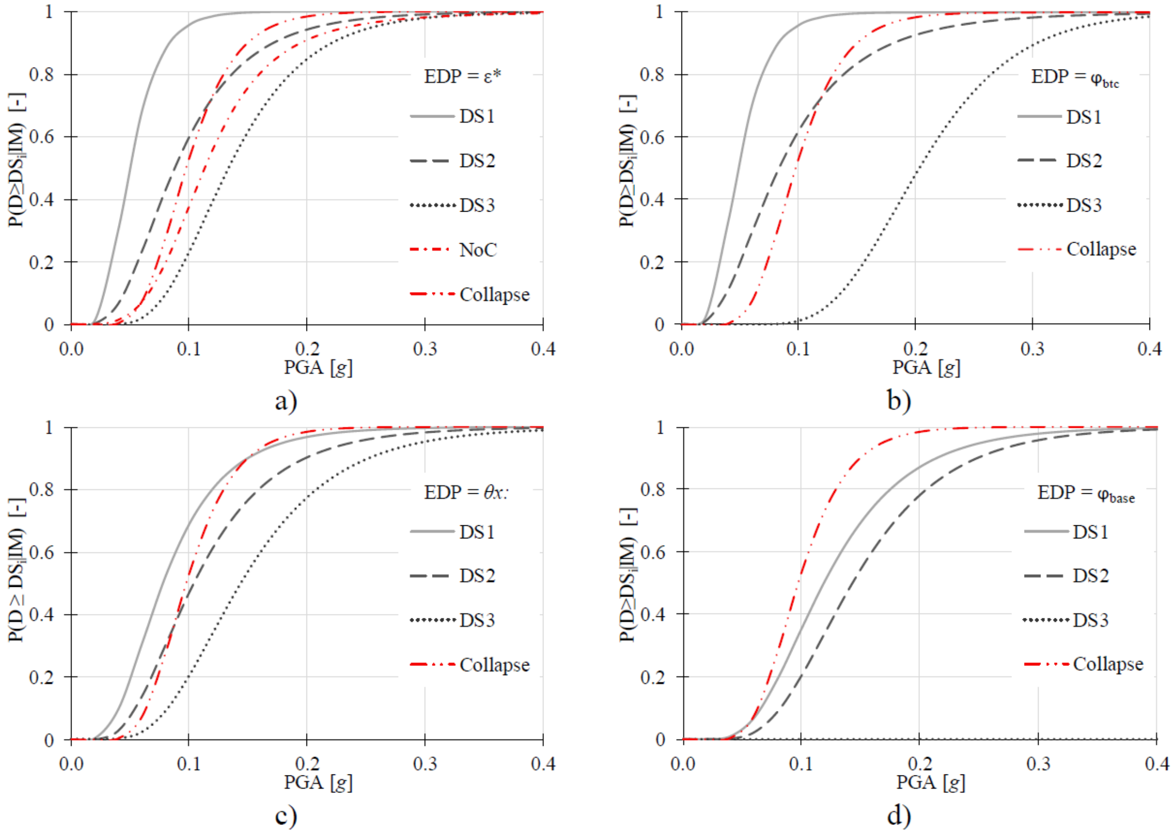

Figure 4: Seismic fragility models conditional on PGA for: ε^{*}, θ_X, φ_{btc}, and φ_{base}.

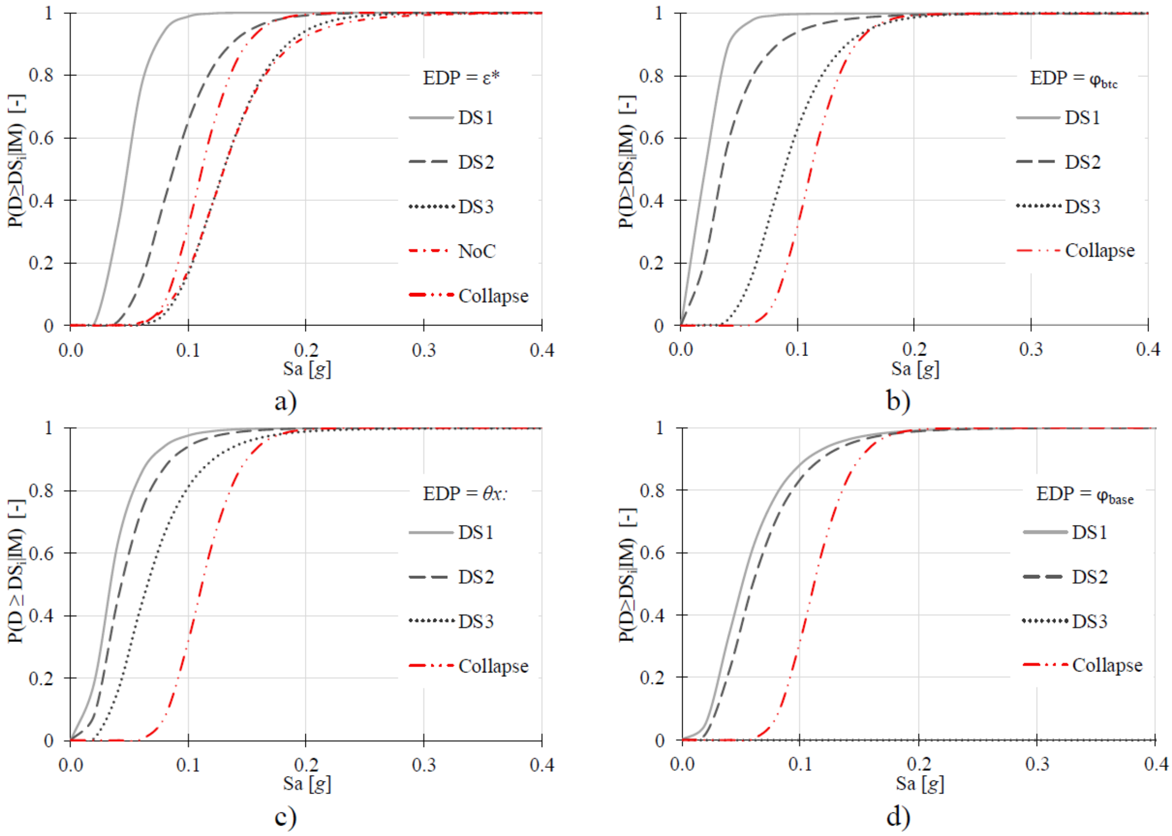

Figure 5: Seismic fragility models conditional on S_a for: ε^{*}, θ_X, φ_{btc}, and φ_{base}.

5 CONCLUSIONS

This study focused on assessing the seismic fragility of 27 unbraced steel pallet racks designed mainly for gravity loads. The rack configurations varied in upright section type (*U*), load-level height (*h*), and total system height (*H*), while maintaining comparable stress levels at the base of the uprights. Specifically, three upright section profiles were considered, combined with three different load-level heights (h = 1, 1.5, and 2 m) and three total rack heights (H = 6, 9, and 12 m).

A dedicated three-dimensional non-linear modelling strategy was developed for these specific storage systems. Beam-to-column (*btc*) and base joints were represented using lumped plasticity models, while the uprights were modelled with distributed plasticity, also accounting for buckling effects. Pallet beams and frame bracing elements were modelled as linear elastic elements. To accurately simulate the reduced stiffness of frames in the cross-aisle direction—due to joint clearances—a reduced equivalent stiffness was applied. A friction-based model was also introduced under each pallet load to account for possible sliding, and the analysis was performed assuming fully loaded conditions.

The fragility assessment was conducted using the Cloud analysis method. A total of 268 unscaled bidirectional ground motion records, representative of Italian seismic conditions on soft or amplifying soils, were employed, leading to 7,236 non-linear time-history (TH) simulations in the OpenSees platform.

Fragility models were developed with respect to two main conventional IMs, i.e., PGA and S_a, considering the following EDPs: a global upright strain measure (ε^*), the load-level drift in the down-aisle direction (θ_X), and the rotational demand at the *btc* (φ_{btc}) and base (φ_{base}) joints about the *Y*-axis. Three damage states (DS1, DS2, and DS3) were defined for each EDP, corresponding to damage onset, yielding, and incipient collapse, respectively. Non-convergent analyses were also incorporated to estimate the actual collapse probability (*Collapse*).

The key findings of the study are summarised below.

- Unbraced pallet racks exhibit significant vulnerability under seismic loading, as indicated by low median values of *Collapse* fragility curves in both PGA and Sa (approximately 0.1 *g*).
- Furthermore, the fragility results obtained for ε^* show that these storage systems have a limited redundancy and ductility capacity, evidenced by the proximity of the fragility curves DS2 (upright yield) and *Collapse*.
- The parameter ε^* emerges as the most representative EDP, as it predominantly governs the collapse mechanism. The θ_X parameter effectively captures the global down-aisle deformation of the rack. The fragility expressed in terms of φ_{btc} indicates that beam-to-column (*btc*) joints are the initial elements to yield, although their failure generally follows that of the uprights. Conversely, the fragility obtained for φ_{base} reveals that base joints are the most resistant to failure.
- While fragility curves based on PGA provide more general insights into the damage and collapse mechanisms of the racks (as they allow the comparison of EDPs associated with different principal directions of seismic action), those based on S_a offer a more direct and specific assessment of the strength and performance of the rack components.

Future research will aim to assess the seismic fragility of additional racking configurations (e.g., pallet racks with spine or vertical bracing), as well as the potential reduction in fragility resulting from seismic retrofit interventions—both conventional and innovative solutions, such as the use of isolation devices.

ACKNOWLEDGMENTS

This work was carried out within the RETURN Extended Partnership and received funding from the European Union Next-GenerationEU (National Recovery and Resilience Plan – NRRP, Mission 4, Component 2, Investment 1.3 – D.D. 1243 2/8/2022, PE0000005).
This study was also partially funded by the Italian Department of Civil Protection, in the framework of the ReLUIS-DPC Project 2024-2026 (Work Package 4, Task 7: Industrial Buildings).

REFERENCES

[1] Perrone, D., Calvi, P. M., Nascimbene, R., Fischer, E. C., Magliulo, G. (2019). "Seismic performance of non-structural elements during the 2016 Central Italy earthquake." Bull Earthq Eng, 17(10): 5655-77.

[2] Donà, M., Bizzaro, L., Carturan, F., and da Porto, F. (2019). "Effects of business recovery strategies on seismic risk and cost-effectiveness of structural retrofitting for business enterprises." Earthq. Spectra, 35(4):1795–1819.

[3] Padilla-Llano, D. A., Moen, C. D., and Eatherton, M. R. (2014). "Cyclic axial response and energy dissipation of cold-formed steel framing members." Thin-walled structures, 78, 95-107.

[4] Padilla-Llano, D. A., Eatherton, M. R., and Moen, C. D. (2016). "Cyclic flexural response and energy dissipation of cold-formed steel framing members." Thin-Walled Structures, 98, 518-532.

[5] Bernuzzi, C., and Castiglioni, C. A. (2001). "Experimental analysis on the cyclic behaviour of beam-to-column joints in steel storage pallet racks." Thin-Walled Structures, 39(10), 841-859.

[6] Zhao, X., Dai, L., and Rasmussen, K. J. (2018). "Hysteretic behaviour of steel storage rack beam-to-upright boltless connections." J. Constr. Steel Res., 144, 81-105.

[7] Proença, J., Rosin, I., and Calado, L. (2009). "Storage racks in seismic areas". European Commission, Directorate-General for Research and Innovation. Publications Office.

[8] Drei, A., Rovere, L., Vayas, I., et al. (2016). "Seismic behaviour of steel storage pallet racking systems (SEISRACKS2): final report". European Commission, Directorate-General for Research and Innovation. Publications Office. https://data.europa.eu/doi/10.2777/686466.

[9] European Racking Federation. (2011). FEM Document 10.2.08. "Recommendations for the design of static steel pallet racks in seismic conditions" – Version 1.04 – May 2011. https://www.fem-rands.org/publications.

[10] CEN (European Committee for Standardization). (2016). "EN 16681. Steel Static Storage Systems – Adjustable Pallet Racking Systems – Principles for seismic design." Brussels: CEN.

[11] Simoncelli, M., Tagliafierro, B., and Montuori, R. (2020). Recent development on the seismic devices for steel storage structures. *Thin-Walled Struct.* 155, 106827. doi:10.1016/j.tws.2020.106827

[12] Shaheen, M. S. A., and Rasmussen, K. J. R. (2022). Development of friction damped seismic fuses for steel storage racks. *J. Constr. Steel Res.* 192, 107216. doi:10.1016/j.jcsr.2022.107216

[13] Donà, M., Bernardi, E., Zonta, A., Ceresara, M. and da Porto, F. (2022). Effectiveness of load-level isolation system for pallet racking systems. *Frontiers in Built Environment*, Volume 8 – 2022. https://doi.org/10.3389/fbuil.2022.944026

[14] Donà M., Bernardi E., Ceresara M., Tan P., and da Porto F. (2024), "Optimization and effectiveness of Load-Level Isolation System (LLIS) for steel pallet racks", in: Jie Yang, Jiyang Fu, A. Liu, A. Ching-Tai Ng (eds.), Proc. of 1st International Conference on Engineering Structures (ICES 2024), Guangzhou, China, November 8-11, 2024. *Lecture Notes in Civil Engineering*

[15] Gabbianelli, G., Francesco, C., and Nascimbene, R. (2020). "Seismic vulnerability assessment of steel storage pallet racks." Ingegneria Sismica, 37(2)

[16] Nuñez, E., Aguayo C., and Mata, R. (2023). "Incremental dynamic analysis of steel storage racks subjected to Chilean earthquakes." Thin-Walled Structures, 182, 110288.

[17] Donà, M., Piredda, G., Zonta, A., Bernardi, E., da Porto, F. (2024). "Seismic fragility of unbraced industrial steel pallet racks." Structural Safety, 110, 102497. https://doi.org/10.1016/j.strusafe.2024.102497

[18] CEN (European Committee for Standardization). (2005). "EN 1993-1-1. Eurocode 3: Design of steel structures – Part 1-1: General rules and rules for buildings." Brussels: CEN.

[19] CEN (European Committee for Standardization). (2020). "EN 15512. Steel Static Storage Systems – Adjustable Pallet Racking Systems – Principles for structural design." Brussels: CEN.

[20] McKenna, F., Fenves, G. L., Scott, M. H. (2000): Open System for Earthquake Engineering Simulation. University of California, Berkeley, CA

[21] Paolucci, R., Ozcebe, A. G., Smerzini, C., Masi, A., and Manfredi, V. (2020). "Selection and spectral matching of recorded ground motions for earthquake engineering analysis." Available at: http://143.225.144.186:5000/

[22] Manfredi, V., Masi, A., Özcebe, A. G., Paolucci, R., and Smerzini, C. (2022). "Selection and spectral matching of recorded ground motions for seismic fragility analyses." Bull Earthq Eng, 1-27.

[23] Saler, E., Carpanese, P., Follador, V., da Porto, F. (2021). "Derivation of seismic fragility curves of a gravity-load designed RC school building through NLTHA." Proc. 8th Inter. Conf. on Computational Methods in Structural Dynamics and Earthquake Engineering, Athens, Greece.

[24] Jalayer, F., Ebrahimian, H., Miano, A., Manfredi, G., Sezen, H. (2017). "Analytical Fragility Assessment Using Unscaled Ground Motion Records." Earth Eng and Struct Dyn, 46 (15), 2639-63.